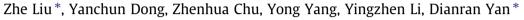
# Materials and Design 52 (2013) 630-637

Contents lists available at SciVerse ScienceDirect

Materials and Design

journal homepage: www.elsevier.com/locate/matdes

# Corrosion behavior of plasma sprayed ceramic and metallic coatings on carbon steel in simulated seawater



School of Materials Science and Engineering, Hebei University of Technology, Tianjin, China

## ARTICLE INFO

Article history: Received 6 April 2013 Accepted 2 June 2013 Available online 15 June 2013

Keywords: Ceramic coating Plasma spray Corrosion Microstructure

## ABSTRACT

 $Al_2O_3$ ,  $ZrO_2$  and Ni60 coatings were produced on carbon steels by plasma spray. Ni60 was used as the bond coat in all the cases. The microstructure of these coatings was analyzed by scanning electron microscopy (SEM). The corrosion behavior of the plasma spray coated samples as well as uncoated samples was evaluated by open circuit potential (OCP) measurements, potentiodynamic polarization tests, and electrochemical impedance spectroscopy (EIS) in simulated seawater. The results showed that Ni60 coating protected carbon steels against the corrosion and plasma spraying ceramic powders on metallic coating improved the corrosion resistance of the coatings further. The corrosion resistance of the  $Al_2O_3$  coating was superior to that of the  $ZrO_2$  coating due to the relatively few defects in  $Al_2O_3$ coating.

© 2013 Elsevier Ltd. All rights reserved.

## 1. Introduction

Nowadays, the carbon steels have been applied extensively due to their high mechanical properties and machine-ability at a low price. However, poor corrosion resistance greatly restricts their further application, especially in aggressive environments (e.g. seawater). Various methods such as cathodic protection, corrosion inhibitor technique and covering the steels with coatings or films are employed to protect the steels against the corrosion [1]. One of the most common routes to decrease the corrosion rate of steel is to deposit a protective coating onto the steel surface [2,3]. The protective coating could be prepared by some kinds of techniques like chemical vapor deposition (CVD), physical vapor deposition (PVD), sol-gel, plasma electrolytic oxidation (PEO) and plasma spray [4-6]. Among these techniques, plasma spraying is one of the most popular methods because it does not cause deterioration of the substrate, and thick coatings (up to hundreds of microns) can be formed at a low cost and high deposition rate [7–9].

Plasma sprayed metallic coating can protect carbon steels against the corrosion [10–12]. The ceramic coatings can work in the environments where both wear and corrosion resistances are required, especially at an elevated temperature; other coatings, such as organic and metallic coatings, cannot compare [13–15]. For example, alumina and zirconia coatings are increasingly and widely used for a range of industrial applications to provide wear

and erosion resistance, corrosion protection and thermal insulation [16,17]. Despite of the fact that the coating materials themselves are highly corrosion resistant, existing defects in plasma sprayed ceramic coatings are detrimental to the corrosion resistance of such coated systems [18–20]. Through-coating defects (e.g. pores) are particularly deleterious as they provide direct paths for corrosive electrolytes to reach the coating/substrate interface [21,22].

Electrochemical impedance spectroscopy (EIS) is a powerful analysis technique and has shown its usefulness to study the localized corrosion of coating/steel systems [23,24]. However, there are few instances of research work on plasma sprayed ceramic coatings in saline solution by EIS technique at present. In this paper, the corrosion process of plasma sprayed coatings during long time immersion was investigated by EIS technique. In addition, the corrosion resistance of carbon steel Q235, samples covered with plasma sprayed ceramic coatings (Al<sub>2</sub>O<sub>3</sub> and ZrO<sub>2</sub>) as well as the metallic coatings (Ni60, for comparison) in simulated seawater were evaluated using the corrosion potential–time curve ( $E_{corr} \sim t$ ) and potentiodynamic polarization, complemented by scanning electron microscopy (SEM).

# 2. Experimental procedures

Q235 carbon steel was used as substrate which was machined into samples of  $10 \text{ mm} \times 10 \text{ mm} \times 15 \text{ mm}$ . Before spraying process the substrate was sand-blasted. The Ni60 powder was plasma sprayed on the treated substrate and also used as a bond coat in all the coatings to provide a rough surface for mechanical bonding of the top coat. Chemical components of Ni60 were as followed (wt.%):  $\leq 0.70\%$ C,  $\leq 2.70\%$ B,  $\leq 3.0\%$  Mo,  $\leq 4.50\%$ Si,  $\leq 5.0\%$ Fe,





Materials & Design

<sup>\*</sup> Corresponding authors. Address: No. 29 Guangrong Road, Hongqiao District, Tianjin 300132, China. Tel.: +86 22 60204810; fax: +86 22 26564810.

*E-mail addresses*: liuzhe1115@163.com, liuzhe1115@hebut.edu.cn (Z. Liu), yandianran@126.com (D. Yan).

<sup>0261-3069/\$ -</sup> see front matter  $\circledast$  2013 Elsevier Ltd. All rights reserved. http://dx.doi.org/10.1016/j.matdes.2013.06.002

 $\leq$ 17.0%Cr and  $\geq$ 60.0%Ni. The size of Al<sub>2</sub>O<sub>3</sub> and ZrO<sub>2</sub> powders was 50–74 µm. The coatings were prepared by plasma spraying equipment, which includes a GP-80 electric power of 80 kW, and a BT-G3 gun manufactured by Taixing Yeyuan Device Company in China. The main spraying parameters are presented in Table 1.

The surface morphology and microstructure of coatings were investigated by a scanning electron microscopy (SEM, S-4800, Hit-achi, Japan), in combination with energy dispersive X-ray analysis (EDAX). The morphology (e.g. defects), coverage and uniformity of the coatings can be directly examined. However, to view the cross-sectional microstructure, fractured cross-sections of the coated steels were prepared as follows: (1) cut with a handsaw from the uncoated side until it is near the substrate/coating interface (1 mm); (2) break the specimen through the pre-cut location. The samples can then be readily examined through SEM. Coating porosity was measured by using the optical microscope coupled with image analysis. The average percentage porosity values were obtained by analyzing 20 fields at a magnification of  $200 \times$  on each sample.

Corrosion test samples were prepared according to ASTM: G1. Prior to the start of all the tests, besides Ni60 coating keeping assprayed state,  $Al_2O_3$  and  $ZrO_2$  coatings were wet ground up to 1000 grit SiC paper. Then, the samples were washed in distilled water and ethanol successively. Finally, they were dried in the warm air.

The copper conducting wires were soldered on the corrosion tested samples surface without coatings. Then, the samples were inset with epoxy resin, leaving only an exposed area of coating of about 1 cm<sup>2</sup>. The electrochemical corrosion tests of coating samples were performed in a three-electrode cell with graphite as the counter electrode, a saturated calomel electrode (SCE) as the reference electrode and coating samples as the working electrode. The electrolyte was simulated seawater and its composition is: 96.5 wt.% H<sub>2</sub>O, 2.73 wt.% NaCl, 0.24 wt.% MgCl<sub>2</sub>, 0.34 wt.% MgSO<sub>4</sub>, 0.11 wt.% CaCl<sub>2</sub> and 0.08 wt.% KCl.

Gamry PCI4/750 integrated electrochemical test equipment was used for the corrosion tests. The polarization curves were generated according to ASTM: G5 with a scan rate of 0.5 mV/s and a scan range of -0.2-0.5 V vs.  $E_{OCP}$  after 1 h immersion. EIS was measured at the open circuit potential of coating samples with signal amplitude of 10 mV rms and a frequency range of 0.01-100,000 Hz. The EIS was fitted and interpreted by EIS fitting software ZSimpWin. After long time immersion, the corroded samples were examined by SEM. Three repeated tests were performed for each set of measurements.

# 3. Results and discussion

## 3.1. Microstructure of coatings

The ground surfaces and fractured cross-sections of  $Al_2O_3$  and  $ZrO_2$  coatings were observed with SEM. As shown in Fig. 1, there are many micro pores, laminar splats and straight columnar grains in both plasma sprayed  $Al_2O_3$  and  $ZrO_2$  coatings, which resemble that of the coatings reported in the literature [15]. Open and closed pores in plasma sprayed coatings can originate from several differ-

Table 1The main plasma spraying parameters.

ent factors. These were partly or totally unmelted particles, inadequate flow or fragmentation of the molten droplets and entrapped gas. High cooling rate of the individual splats and poor interlamellar bonding resulted in vertical and horizontal voids, namely cracks. For Al<sub>2</sub>O<sub>3</sub> coating, the defects were mainly in the form of micro pores, and no visible micro cracks were found in it. The pores and cracks in ZrO<sub>2</sub> coating were relatively more and larger. This was confirmed by the porosity values obtained from image analysis measurement for the Al<sub>2</sub>O<sub>3</sub> and ZrO<sub>2</sub> coatings, which were 7% and 9%, respectively. Indeed, this result was in agreement with that of the previous study by Sarikaya, which found that average porosity levels of the Al<sub>2</sub>O<sub>3</sub> coatings ranged from 8.7% to 5.8% [16]. On one hand, this can be attributed to the high melting point of ZrO<sub>2</sub> coating. Although higher torch efficiency was supplied during plasma spraying process, some unmelted loose feedstocks were retained in ZrO<sub>2</sub> coating as marked by arrows (in Fig. 1d). On the other hand, the thermal conductivity of alumina is higher than that of zirconia, and therefore, the alumina powders are more efficiently molten than zirconia in the plasma spraying. These structural defects were more detrimental to the corrosion performance, as they provided direct paths to allow the corrosive electrolyte to access the steel substrate.

As-sprayed surface and cross-section of Ni60 coating were also observed with SEM. As shown in Fig. 2, Ni60 powders were well molten and the major parts of Ni60 bond coating were relatively compact, however, there were also some defects in its surfaces and cross-sections. It was found that Ni60 bond coatings were well-bonded to both the coatings and substrate with no distinctive irregular interface.

### 3.2. Corrosion behavior of coatings in simulated seawater

### 3.2.1. $E_{corr} \sim t$ curves

The measurement of  $E_{corr}$  as a function of immersion time is used to study some aspects of the chemical stability and corrosion process of the coatings. The  $E_{corr} \sim t$  curves of the Al<sub>2</sub>O<sub>3</sub>, ZrO<sub>2</sub> and Ni60 coatings in simulated seawater are shown in Fig. 3. For comparison, the  $E_{corr}$  of uncoated Q235 carbon steel is also recorded and presented in the same figure. The high value of the potential for all of these coatings at the beginning of immersion could be explained by the time necessary for the solution to reach the substrate by the diffusion and penetration through the pinholes and pores in the surface. Soon after this, the potential decreased gradually with immersion time before achieving equilibrium potential in simulated seawater. However, the slope of  $E_{corr}$  for Ni60 coatings and Q235 carbon steel was much gentle than that of Al<sub>2</sub>O<sub>3</sub> and ZrO<sub>2</sub> coatings. This behavior was associated with less porous structure of the metallic coating compared to the ceramic coatings.

 $Al_2O_3$ ,  $ZrO_2$  and Ni60 coatings were chemically relatively inert, and consequently, had a quite noble corrosion potential, which was more positive than that of Q235. In such a system, where a relatively noble cathode (coating) lay over a less noble substrate of small area (Q235), corrosion was expected to initiate rapidly. The extent of the corrosion rate depended on the pinholes and pores on the coating surface. Ni60 coating can provide corrosion protect for the substrate. This result agreed with that obtained by Liu et al.,

Powder type	Voltage (V)	Current (A)	Torch efficiency (kW)	Spraying distance (mm)	Gas flow rate (L/min)	
					Ar	H <sub>2</sub>
Ni60	60	500	30	100	80	130
$Al_2O_3$	60	500	30	80-150	70-80	130
ZrO <sub>2</sub>	70	500	35	80-150	70-80	150

Download English Version:

https://daneshyari.com/en/article/7221303

Download Persian Version:

https://daneshyari.com/article/7221303

Daneshyari.com